

Dear Reviewer,

We sincerely thank the reviewer for careful evaluation of our manuscript and for providing insightful and constructive comments. We appreciate the recognition of our work and the suggestions offered to improve its clarity and scientific rigor. In the responses below, the reviewer's original comments are reproduced in *italic* for clarity. Our point-by-point replies follow each comment and are marked in green. All corresponding changes have been made in the revised manuscript and are marked in blue. Line numbers refer to the revised manuscript unless otherwise noted.

*This paper presents the ambient OOMs measurement in a complex urban environment in China. By combining binPMF with multiple sub-range spectral analysis, 2571 OOMs were successfully identified, 11 distinct factors were used to explain major OOM formation pathways: five daytime photochemical processes, four nighttime NO<sub>3</sub>-driven oxidation processes, and two regional mixed sources. This analysis achieved the first successful separation of sesquiterpene oxidation products in environmental measurements. In previous studies, these compounds were indistinguishable in traditional full-spectrum analyses due to their weak signals and overlapping temporal patterns with other nocturnal factors. In general, I think this paper is well-structured and easy to follow. However, I do have some concerns that need to be addressed before it can be accepted for publication.*

**Major Comments:**

**1. Clarifications on Factor Analysis in R1, R2, and R3**

*In Figure 3, R1, R2, and R3 correspond to 6, 8, and 9 factors, respectively, whereas Figures S2-S4 in the SI indicates that 12 factors are required to explain the N2-MT-I factors in R1, and 11 factors are needed for both R2 and R3.*

*(a) Figure S2 shows 5 NP-related factors, and Figure S3 shows 2 NP-related factors.*

*Since the formation pathways of these ions were not discussed in the final analysis, would it be possible to re-perform the factor analysis after removing the NP-related ions?*

**Response:**

Thank you for the constructive suggestion. To evaluate the influence of NP-related ions on our factor analysis, we removed the major NP-related bins from the original mass spectra (e.g., the bins near 201 Th for C<sub>6</sub>H<sub>5</sub>NO<sub>3</sub>NO<sub>3</sub><sup>-</sup>) and re-performed the binPMF analysis. It is important to note that only bins associated with high-abundance NP signals were removed. Bins associated with lower-abundance NP species were retained, as they may be adjacent to non-NP OOMs with similar masses, and removing them could lose valuable information. The updated analysis yielded a new 8-factor solution (Fig. R1), which we compared with the original solution through correlation analysis (Fig. R2).

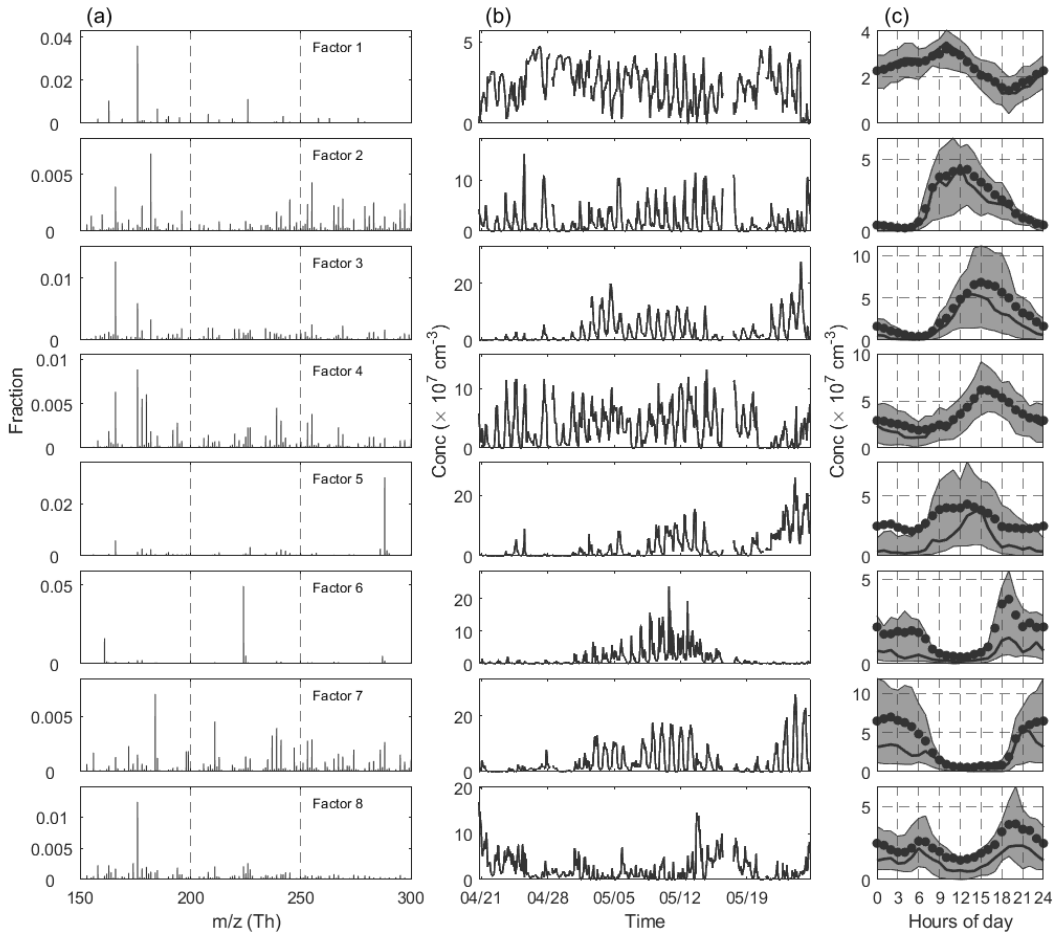


**Figure R1.** Selected binPMF solution for Range 1 after removing NP-related bins. (a) PMF factor profiles. (b) Time series of these factors. (c) Diurnal variations in PMF factors.

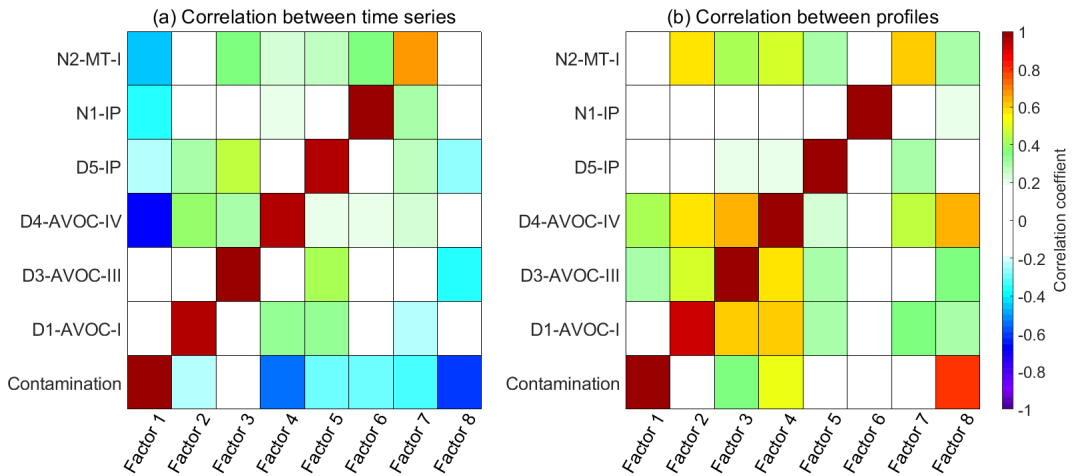


**Figure R2.** Comparison of the new 8-factor solution (after removal of NP-related bins) with the original solution. (a) Correlation of factor time series, and (b) correlation of factor profiles.

We found that all seven non-NP-related factors from the original solution were well reproduced. The additional factor (Factor 8) in the new solution consists primarily of perfluorinated acids and the residual NP-related ions. Unlike high-resolution PMF where individual ions can be excluded, our binPMF method operates directly on the raw spectral matrix. Therefore, to eliminate the influence of specific compounds, the corresponding mass spectral bins need to be removed. In this case, removing only the most prominent NP-related peaks resulted in the loss of nearly 2000 bins, which leads to a notable reduction in the spectral information available for analysis. Given this, we chose to retain the NP-related signals in our final analysis. In previous studies at our site (Liu et al., 2021, 2023), we also performed binPMF analysis and successfully separated NP-related factors. These studies consistently reveal their distinct chemical signatures compared to other OOMs. Because of these differences, NP-related components are usually resolved into individual factors with minimal overlap with other factors. Therefore, their exclusion in the current analysis is not expected to affect the overall factor resolution or interpretation. We have added this clarification to Line 247-261 in the revised manuscript for transparency.

Revised text:

**Page 7, Line 247-261:** In total, 17 merged factors are identified. These include five factors associated with daytime chemistry (denoted by the "D-" prefix), four factors linked to nighttime chemistry ("N-" prefix), two factors with no significant diurnal patterns and six factors excluded from the following discussion. Of these six disregarded factors, five factors are dominated by nitrophenol-related compounds, and one is characterized by fluorinated contaminants. The nitrophenol (NP) factors are not further analyzed in this study, as they have been extensively investigated in previous work (Cheng et al., 2021; Song et al., 2021; Chen et al., 2022). At this site, earlier binPMF analyses successfully separated NP factors (Liu et al., 2021, 2023), revealing their distinct chemical signatures compared to other OOMs. Due to these clear distinctions, NP-related components are typically resolved into separate factors with minimal overlap. Therefore, their exclusion in the current analysis is not expected to affect the overall factor resolution or interpretation. The contamination factor is primarily composed of various fluorinated compounds, mainly perfluorinated organic acids, which originated from the Teflon tubing used in our sampling system.

*(b) Could you provide a detailed explanation of the contamination factors present in R1, R2, and R3?*

**Response:**

We appreciate the reviewer's question regarding the contamination factors observed in the three mass spectral subranges. In all three ranges (R1, R2, and R3), one factor is consistently dominated by fluorinated compounds, accounting for approximately 65% of the total signal intensity in that factor. These compounds are primarily identified as various types of fluorinated organic compounds, which were introduced from the sampling system, most likely through the Teflon tubing used in the instrument setup.

The major compounds in this factor are shown in the Fig. R3. The main molecular structures feature perfluoroalkyl chains—in which all C-H bonds are replaced by C-F bonds—bearing one or two oxygen-containing functional groups (e.g., carboxyl, hydroxyl, or aldehyde). Representative examples include  $C_xF_{2x+1}COOH$ ,  $C_xF_{2x+1}OH$ , and  $C_xF_{2x}CH_2O_2$ .

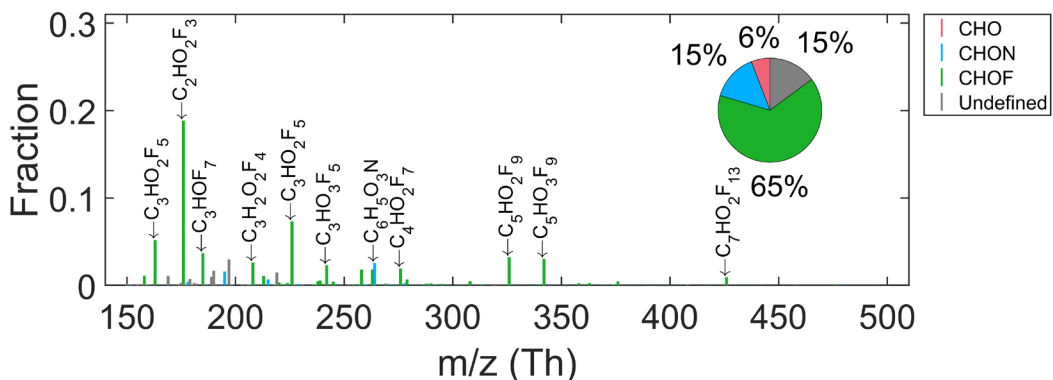


**Figure R3.** Mass spectra of the Contamination factor. The elemental formulas of major peaks are labeled above them. Peaks are colored by compound classes as indicated in the legend, and the fractions of peaks grouped by compound classes are reported in the pie chart.

(c) In R3, the factors D3-AVOC-III-1 and D3-AVOC-III-2 were merged before conducting correlation analysis with factors in the first two ranges. Could you elaborate on how this merging was specifically performed?

**Response:**

The merging was performed as follows:

First, the time series of the two factors were summed to create the time series (ts) of the new merged factor. Then, the original time series and profiles of each factor were used to reconstruct their respective data matrices ( $A_1$  and  $A_2$ ) by matrix multiplication. These two matrices were then added to obtain the data matrix A of the combined factor:

$$A = A_1 + A_2 = (ts_1 \cdot pr_1) + (ts_2 \cdot pr_2) \quad Eq. R1$$

Finally, the new profile (pr) of the merged factor was derived by solving the equation:

$$ts \cdot pr = A \quad Eq. R2$$

This approach preserved both the temporal and spectral information of the original two factors and ensured consistency in subsequent correlation analysis across subranges.

We have included the above relevant descriptions in the supplement.

## 2. Interpreting OOM Factors Based on Precursor Compounds

CIMS data typically utilizes fingerprint molecules to characterize formation pathways. However, in complex atmospheric environments, naming factors based on

their precursors (e.g., AVOC, isoprene, monoterpane) introduces significant interpretation challenges. For instance, regarding the D1-AVOC-I factor, the currently presented evidence collectively supports its interpretation:

*It correlates relatively well with the 'Arom $\times$ OH' proxy.*

*This factor exhibits the highest average double bond equivalent (DBE).*

*The tracer molecules show comparability with existing laboratory studies.*

*For other factors, could additional discussion of results be incorporated in Sections 3.2 and 3.3? Specific comments follow:*

*(a) [D2-AVOC-II] Lines 291-292: "The first series represents typical aliphatic products, while the latter corresponds to second-generation aromatic products observed in laboratory studies." Please provide the reference/supporting evidence for this statement. Furthermore, it cannot be denied that  $C_xH_{2x-2}O_8N_2$  (e.g., C=10) may also originate from terpene oxidation (Luo et al., 2023).*

**Response:**

We sincerely thank the reviewer for pointing out the limitations in our original statement. We agree that the previous wording regarding the interpretation of D2-AVOC-II was overly assertive and lacked sufficient supporting evidence. As suggested, we have revised the relevant description in the manuscript (Lines 336–342) to improve accuracy and clarity. Specifically, we have toned down the language and added supporting references from laboratory studies to substantiate the identification of second-generation aromatic products. In addition, we have incorporated the reviewer's important observation that compounds such as  $C_{10}H_{18}O_8N_2$  (i.e.,  $C_xH_{2x-2}O_8N_2$  with x = 10) could also originate from terpene oxidation, as demonstrated in Luo et al. (2023). This possibility was indeed overlooked in the original manuscript, and we have now acknowledged it explicitly in the revised text:

Revised text:

**Page 11, Line 336-342:** The first series also account for a substantial fraction in the Aliph-OOM factor in the summertime at this site (Liu et al., 2021). These near-saturated compounds are likely oxidation products of aliphatic precursors under strong NO<sub>x</sub> influence in urban air, as proposed in previous laboratory studies (Algrim and Ziemann, 2019; Wang et al., 2021). Notably, it cannot be denied that  $C_{10}H_{18}O_8N_2$  may also originate from terpene oxidation (Luo et al., 2023). The latter corresponds to second-generation aromatic products observed in laboratory studies (Tsiliannis et al., 2019; Wang et al., 2020).

We appreciate this valuable suggestion, which has helped improve the robustness and balance of our factor interpretation.

*(b) [D3-AVOC-III] Line 306: "These compounds are typical aromatic oxidation products." This conclusion appears overly assertive, as these products— $C_xH_{2x-4}O_5$*

(7.3% abundance) and  $C_xH_{2x-2}O_5$  (6.0% abundance)—could also potentially originate from isoprene and monoterpene oxidation.

**Response:**

We appreciate the reviewer's comment and fully agree that the original statement was overly definitive. As noted, compounds such as  $C_xH_{2x-4}O_5$  and  $C_xH_{2x-2}O_5$  may also originate from the oxidation of isoprene and monoterpenes. In fact, similar factors have been reported in other ambient PMF studies. For example, Massoli et al. (2018) identified an "isoprene afternoon" factor at a forested site, while Yan et al. (2016) described a "Daytime type-3" factor, and Liu et al. (2021) observed a "Temp-related" factor in an urban environment. These factors exhibited strong correlations with temperature and were hypothesized to be associated with low- $NO_x$  daytime oxidation of isoprene or fragment products from monoterpene oxidation. However, based on the relatively high DBE values and the large contributions from C6–C8 compounds observed in this factor, we tend to attribute it predominantly to anthropogenic aromatic precursors. We have revised the manuscript accordingly (Lines 365–372) to reflect a more cautious interpretation and now present this factor as likely influenced by aromatic compounds but potentially containing contributions from biogenic sources as well:

Revised text:

**Page 12, Line 365-372:** While their high DBE values and relatively high contributions from C6-C8 species suggest a strong influence from aromatic oxidation, we acknowledge that contributions from isoprene and monoterpene oxidation under low- $NO_x$  conditions cannot be ruled out. Similar factors were identified in previous studies, including an "isoprene afternoon" factor at a forest site in Alabama (Massoli et al., 2018), a "Daytime type-3" factor at a rural site in Finland (Yan et al., 2016), and a "Temp-related" factor in an urban environment (Liu et al., 2021), all showing temperature dependence and potential biogenic influence.

**Page 12, Line 382-384:** Therefore, we propose this factor represents a characteristic photochemical process associated with  $O_3$  formation, dominated by anthropogenic VOCs, but with possible contributions from biogenic sources as well.

We thank the reviewer again for this important observation, which has led to a more nuanced and evidence-based discussion of this factor.

(c) [D4-AVOC-IV] The fingerprint molecules  $C_xH_{2x-2}O_4$  and  $C_xH_{2x-1,2x-3}O_6N$  are currently grouped within the same factor. However, are there laboratory studies showing shared precursors for these compounds or similar formation pathway?

**Response:**

Thank you for this insightful comment. We agree that the co-occurrence of these molecular families requires careful interpretation. Although the formation mechanism of this factor is still under investigation, we propose that  $C_xH_{2x-2,2x-4}O_4$  and  $C_xH_{2x-1,2x-3}O_6N$

$\text{C}_x\text{H}_{2x-1}\text{O}_6\text{N}$  can be produced from a common  $\text{RO}_2$  precursor ( $\text{C}_x\text{H}_{2x-1}\text{O}_5$ ) through different reaction branches with  $\text{NO}$ . Specifically,  $\text{C}_x\text{H}_{2x-2}\text{O}_4$  compounds may form via the  $\text{RO}$  pathway, leading to carbonyl products, while  $\text{C}_x\text{H}_{2x-1}\text{O}_6\text{N}$  compounds are typically formed via direct reaction of  $\text{RO}_2$  with  $\text{NO}$  to yield organic nitrates  $\text{RONO}_2$ . Furthermore, a similar relationship is observed between  $\text{C}_x\text{H}_{2x-3}\text{O}_6\text{N}$  and  $\text{C}_x\text{H}_{2x-4}\text{O}_4$ , another group present in this factor (6.6%, Table S4), and  $\text{C}_x\text{H}_{2x-2}\text{N}_2\text{O}_8$  (4.8%, Table S4) found in the R2 range. These observations suggest that these species may indeed share precursors and form via alternative  $\text{RO}_2$  termination channels influenced by  $\text{NO}$  levels. These two branches result in products differing by one  $\text{HNO}_2$  unit, suggesting a mechanistic link. A similar distribution of carbonyls and organic nitrates has been observed in laboratory experiments of alkane oxidation with added  $\text{NO}$ , supporting our interpretation (Wang et al., 2021). We have added this discussion in the revised manuscript (Lines 394–421) and clarified that, while the exact mechanisms remain uncertain, existing evidence supports the plausibility of a shared precursor-based formation for these compounds:

Revised text:

**Page 12, Line 394-421:** While direct laboratory evidence linking these molecular series to a common formation pathway is limited, theoretical considerations and recent chamber studies support their possible co-generation. Both  $\text{C}_x\text{H}_{2x-2}\text{O}_4$  and  $\text{C}_x\text{H}_{2x-1}\text{O}_6\text{N}$  can be derived from the same  $\text{RO}_2$  precursor ( $\text{C}_x\text{H}_{2x-1}\text{O}_5$ ) through different termination pathways with  $\text{NO}$ . The former may form via  $\text{RO}$  radical intermediates ( $\text{C}_x\text{H}_{2x-1}\text{O}_4$ ) that undergo further oxidation to produce carbonyl-containing compounds, whereas the latter results from direct  $\text{NO}$  addition to  $\text{RO}_2$  forming  $\text{RONO}_2$ . The mass difference between these products corresponds to a loss of one  $\text{HNO}_2$  unit. A similar relationship applies between  $\text{C}_x\text{H}_{2x-4}\text{O}_4$  (Table S4) and  $\text{C}_x\text{H}_{2x-3}\text{O}_6\text{N}$ , as well as  $\text{C}_x\text{H}_{2x-2}\text{N}_2\text{O}_8$  in R2. Recent laboratory experiments investigating the  $\text{OH}$  oxidation of alkanes under varying  $\text{NO}$  levels also observed concurrent production of carbonyl species and organic nitrates, supporting this mechanistic linkage (Wang et al., 2021). These observations reinforce the idea that the co-occurrence of these compounds in the same factor likely reflects different chemical pathways stemming from shared precursors.

(d) Line 351: What is the relative importance of ozonolysis for these nighttime factors?

**Response:**

We thank the reviewer for this insightful comment regarding the potential role of ozonolysis in the formation of nighttime OOM factors. Our measurements at this site indicate that nighttime ozone concentrations often remain elevated, as shown in the Fig. S8a.

To better assess the relative importance of ozonolysis, we compared the nighttime (18:00–0:00 LT) reactivities ( $P = k[\text{oxidant}][\text{VOC}]$ ) of  $\text{O}_3$  and  $\text{NO}_3$  toward selected BVOCs, including isoprene (IP) and  $\alpha$ -pinene (MT). Here,  $k$  values were obtained from the Master Chemical Mechanism (MCM v3.3.1; <http://mcm.york.ac.uk/>, last access: 20 June 2025), and due to the lack of direct  $\text{NO}_3$  measurements at this site, its concentration

was simulated using the Framework for 0-D Atmospheric Modeling (F0AM) (Wolfe et al., 2016). The results are presented in Fig. S8b.

We found that for IP and MT,  $\text{NO}_3$ -driven chemistry clearly dominates over ozonolysis, owing to much higher reaction rate constants of  $\text{NO}_3$  (3–5 orders of magnitude greater than those of  $\text{O}_3$ ), even though  $\text{O}_3$  concentrations are higher than those of  $\text{NO}_3$  at night.

In addition, the molecular composition of these nighttime factors further supports the dominance of  $\text{NO}_3$  chemistry. All four nighttime factors exhibit a high proportion of organic nitrate species (>80%), which are unlikely to originate from ozonolysis alone.  $\text{O}_3$ -induced formation of organic nitrates typically requires the presence of NO, which remains at low levels during nighttime at our site.

Furthermore, each nighttime factor contains distinct  $\text{RO}_2$  radicals that are characteristic of  $\text{NO}_3$ -driven oxidation:  $\text{C}_5\text{H}_8\text{O}_5\text{N}$  (from isoprene),  $\text{C}_{10}\text{H}_{16}\text{O}_x\text{N}$  (from monoterpenes), and  $\text{C}_{15}\text{H}_{24}\text{NO}_x$  (from sesquiterpenes). In contrast, we did not observe  $\text{RO}_2$  species commonly associated with ozonolysis pathways, such as  $\text{C}_{10}\text{H}_{15}\text{O}_x$  or  $\text{C}_{15}\text{H}_{23}\text{O}_x$ , which have been reported in laboratory studies of  $\text{O}_3$ –BVOC reactions (Kirkby et al., 2016; Richters et al., 2016; Dada et al., 2023).

These findings further support the conclusion that  $\text{NO}_3$  oxidation plays the dominant role in driving nighttime OOM formation at our site. However, we cannot rule out a potential contribution from ozone oxidation, given the relatively high ozone concentrations observed during the night. We have incorporated this discussion into the revised manuscript, with additional supporting figure and references.

Revised text:

**Page 13, Line 443-447:** However, considering that ozone concentrations remain relatively high during nighttime at this site (Fig. S8a), we cannot exclude a potential contribution from ozonolysis. The following four factors exhibit clear chemical signatures associated with biogenic volatile organic compounds (BVOCs) and their nighttime oxidation, with  $\text{NO}_3$  chemistry playing a dominant role.

**Page 14, Line 515-518:** Nevertheless, given the high reactivity of sesquiterpenes toward ozone (Gao et al., 2022), and the elevated nighttime  $\text{O}_3$  concentrations observed at this site (Fig. S8a), we cannot rule out a potential contribution from ozonolysis.

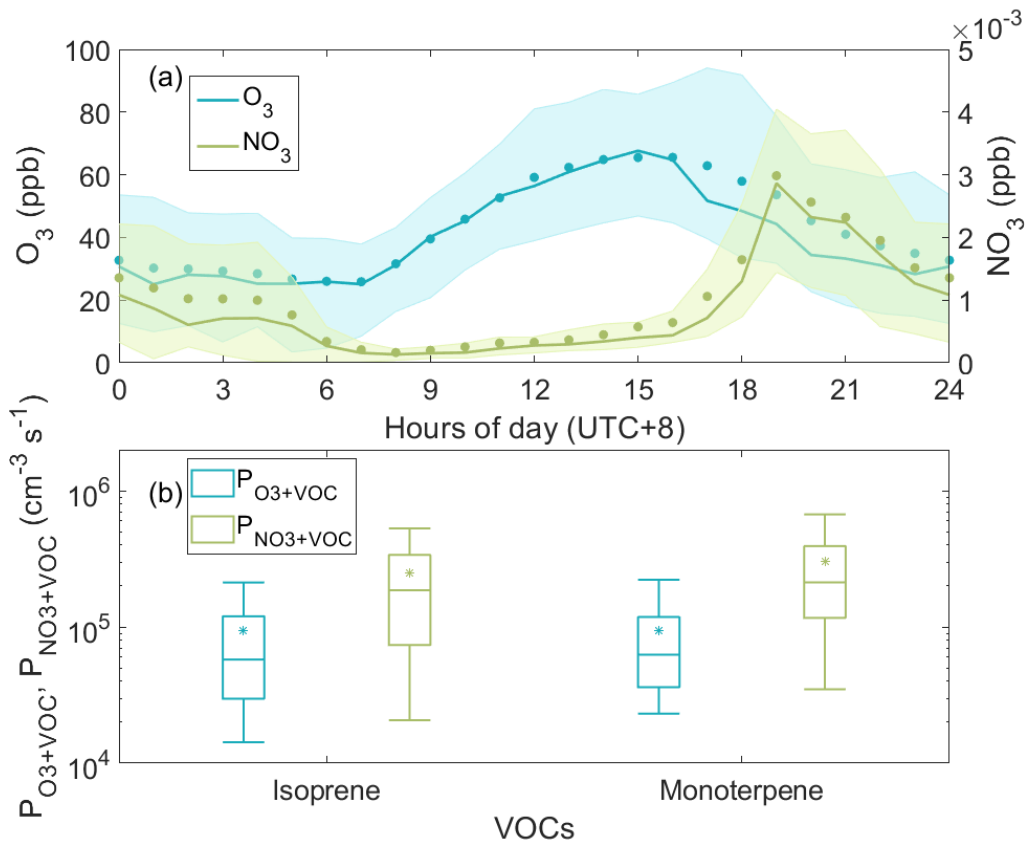


**Figure S8.** (a) Diurnal variations of O<sub>3</sub> and NO<sub>3</sub> radical. (b) Box plot of the oxidation reaction rates of isoprene and monoterpenes by O<sub>3</sub> and NO<sub>3</sub> radical at nighttime.

(e) [NI-IP] Given that the RO<sub>2</sub> radical C<sub>5</sub>H<sub>8</sub>NO<sub>5</sub> accounts for 57.4% of the total factor intensity, while no higher-oxygen-number isoprene-RO<sub>2</sub> radicals were detected, here recommend to plot the time series of C<sub>5</sub>H<sub>8</sub>NO<sub>5</sub> and demonstrate its correlation with the factor.

**Response:**

We appreciate the reviewer's suggestion. To address this, we have added a figure (Fig. S9) showing the time series of C<sub>5</sub>H<sub>8</sub>NO<sub>5</sub> (derived from direct peak fitting without binPMF) alongside the N1-IP factor concentration, as well as a scatter plot of their correlation. As shown, the time series of C<sub>5</sub>H<sub>8</sub>NO<sub>5</sub> closely follows the temporal trend of the N1-IP factor. The Pearson correlation coefficient reaches 0.98, confirming that C<sub>5</sub>H<sub>8</sub>NO<sub>5</sub> serves as a representative tracer for this factor.

Revised text:

**Page 14, Line 458-460:** A peak-fitted time series of C<sub>5</sub>H<sub>8</sub>O<sub>5</sub>N was extracted and compared to the time series of the N1-IP factor. As shown in Fig. S9, the two are highly correlated ( $R = 0.98$ ), demonstrating that this compound can serve as a representative tracer for this factor.

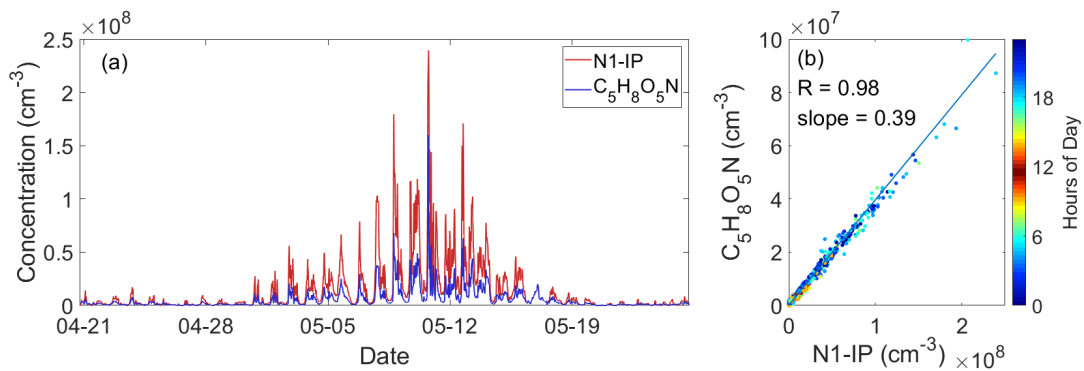


**Figure S9.** Time series and correlation analysis between the N1-IP factor and C<sub>5</sub>H<sub>8</sub>O<sub>5</sub>N. (a) Temporal evolution of the N1-IP factor (red) and C<sub>5</sub>H<sub>8</sub>O<sub>5</sub>N (blue) obtained from direct peak fitting. (b) Correlation between C<sub>5</sub>H<sub>8</sub>O<sub>5</sub>N and the N1-IP factor, colored by hours of day.

(f) [N3-MT-II] From the diurnal pattern, the formation of this factor can be affected by O<sub>3</sub> oxidation.

**Response:**

Thank you for the insightful comment. We agree that the formation of the N3-MT-II factor is likely influenced by multiple oxidants, and ozonolysis may indeed contribute to some extent.

As discussed in Section 2 (d), although O<sub>3</sub> is present at relatively high levels during nighttime at this site, the calculated reaction rate indicates that O<sub>3</sub> oxidation of monoterpenes is significantly slower than NO<sub>3</sub> oxidation.

Furthermore, 98% of the compounds in this factor are organic nitrates, and 84% of them contain two or more nitrogen atoms (Fig. 4). Given the low nighttime NO concentrations at our site, it is difficult for these compounds to be formed efficiently through successive ozonolysis and NO termination steps. Such a pathway is therefore unlikely to be a major contributor to this factor.

Finally, according to current mechanisms, O<sub>3</sub> + monoterpene reactions followed by NO addition are expected to produce C<sub>10</sub>H<sub>15</sub>NO<sub>x</sub> and C<sub>10</sub>H<sub>14</sub>N<sub>2</sub>O<sub>x</sub>, where the DBE remains unchanged from the precursor (DBE = 3). In contrast, the compounds in this factor are characterized by DBE < 3 (Table S9), which is inconsistent with typical O<sub>3</sub> oxidation products. Taken together, we interpret the N3-MT-II factor as a product of multi-oxidant chemistry involving NO<sub>3</sub>, OH, and possibly O<sub>3</sub>, particularly at the day-night transitions. For example, nighttime NO<sub>3</sub>-initiated products may undergo further OH or O<sub>3</sub> oxidation after sunrise, or vice versa. The high abundance of multi-nitrates in this factor supports the idea of sequential oxidation steps under varying oxidant conditions. We have clarified this point in the revised manuscript to avoid any ambiguity.

**Revised text:**

**Page 14, Line 493-503:** This suggests that  $\text{NO}_3$ -initiated oxidation of monoterpenes at night is followed by further oxidation in the morning, potentially involving  $\text{OH}$  and  $\text{O}_3$ , leading to the observed multi-nitrate species. Furthermore, some of the nighttime concentrations may arise from daytime oxidation products that undergo additional  $\text{NO}_3$ -driven oxidation during the night. Overall, this factor represents multi-generational oxidation products, involving various oxidants during the transition between day and night.

(g) [Mixed-MT] The current characterization of this factor appears incomplete and need additional explanation.

**Response:**

We agree that the characterization of the Mixed-MT factor could benefit from further clarification. We have revised the manuscript to provide additional discussion on its chemical composition and potential formation pathways.

Revised text:

**Page 16, Line 551-567:** This factor exhibits a complex molecular composition with a broad carbon number distribution ( $\text{C}_5\text{-C}_{15}$ ), suggesting contributions from multiple precursor classes. While monoterpene-derived dinitrates ( $\text{C}_{10}\text{H}_{16}\text{O}_{8,9}\text{N}_2$ ,  $\text{C}_{10}\text{H}_{18}\text{O}_8\text{N}_2$ ) dominate the composition and indicate multi-generational oxidation, the presence of a wide range of oxidation products implies the involvement of both biogenic and anthropogenic sources. Notably, the most abundant compounds in R2 are  $\text{C}_x\text{H}_{2x-3,2x-5}\text{O}_6\text{N}$ , while in R3, the corresponding species are mainly  $\text{C}_x\text{H}_{2x-2,2x-4}\text{O}_8\text{N}_2$  (Table S11), differing by one  $\text{HNO}_2$  group. This pattern closely resembles that observed in the D4-AVOC-IV factor, further supporting the involvement of  $\text{NO}$  in the formation pathways. The high organic nitrate fraction (84%) further supports this interpretation. Taking the  $\text{C}_{10}$  compounds as an illustrative example, species such as  $\text{C}_{10}\text{H}_{17}\text{NO}_{5-8}$  are consistent with  $\text{OH}$  oxidation products of  $\alpha$ - and  $\beta$ -pinene observed in laboratory studies, while  $\text{C}_{10}\text{H}_{18}\text{N}_2\text{O}_{8,9}$  are likely formed through subsequent generation reactions. Additionally, the presence of  $\text{C}_{10}\text{H}_{15}\text{NO}_{5-7}$  suggests a contribution from  $\text{O}_3$ -initiated oxidation pathways. Altogether, these observations imply that this factor reflects a mixture of oxidation processes involving both  $\text{OH}$  and  $\text{O}_3$ , rather than being dominated by a single oxidant or precursor type.

### 3. Mixed-Precursor Effects on Volatility Estimation

In the discussion of OOM volatility, the authors state: "The identification of monoterpene-related compounds was based on the approach proposed by Nie et al. (2022), where OOMs with  $\text{DBE}=2$  that appeared in the PMF monoterpene-related factors were classified as monoterpene OOMs." This precursor-dependent classification approach introduces additional uncertainty to the volatility distribution

shown in Figure 5, particularly for factors like Mixed-MT where precursors are not exclusively monoterpenes.

**Response:**

Thank you for pointing this out. We acknowledge that the original description of our classification method was unclear and contained a misstatement. In our analysis, we adopted a modified version of the classification proposed by Nie et al. (2022), in which terpene-related OOMs were identified within the terpene-dominated PMF factors (N2-MT-I, N3-MT-II, N4-SQT, and Mixed-MT). Specifically, we classified compounds as terpene OOMs with DBE between 2 and 4. For these terpene OOMs, we estimated their saturation vapor concentrations using the parameterization proposed by Mohr et al. (2019), which considers the influence of hydroperoxide on volatility.

We agree that this precursor-based classification remains a simplified approach and introduces some degree of uncertainty, particularly for mixed-source factors such as Mixed-MT. In urban environments, distinguishing terpene oxidation products from those originating from aromatic VOCs remains challenging, and the volatility estimates for such factors are subject to potential overlaps and misclassifications.

To further evaluate the effect of this classification on volatility distributions, we included an additional analysis (Fig. R4) comparing the resulting volatility distribution used in our study (VBS 1) with an alternative scheme (VBS 2) where all OOMs were treated using the Mohr method. The differences between the two schemes illustrate the uncertainty introduced by precursor-based volatility classification, but also fall within the expected range of variation caused by using different, yet reasonable, parameterizations. Although this factor is of mixed origin, we believe that monoterpenes still represent the dominant contributor, and therefore applying this volatility correction provides a more realistic representation than using a generic parameterization for all components.

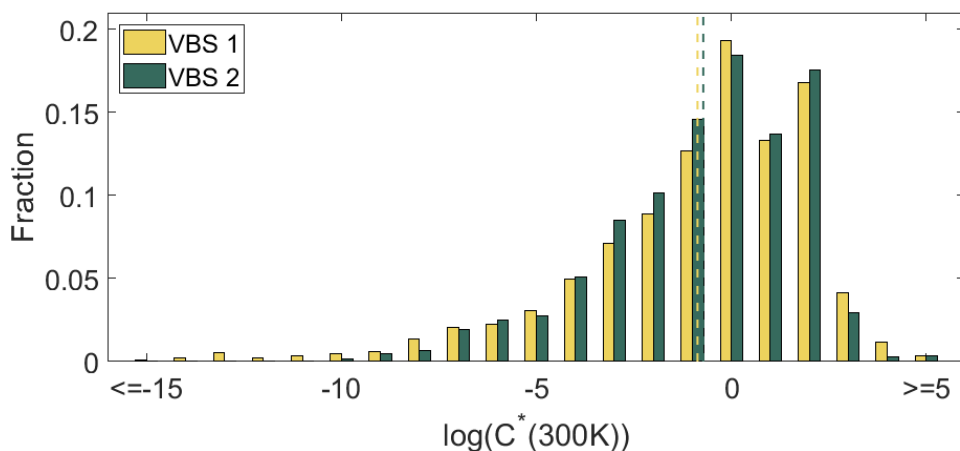


**Figure R4.** Comparison of volatility distributions ( $\log C^*$  at 300 K) for the Mixed-MT factor using two different methods for estimating saturation concentration. The dashed lines indicate the mean  $\log C^*$  values for each method.

**Minor Comment:**

Line 192:  $C_6H_5OHNO_3$ - is incorrect.

Line 306: should be Table S3.

**Response:**

Thank you for pointing these out. We have corrected the molecular formula and updated the reference to Table S3 in the revised manuscript.

**Reference:**

Algrim, L. B. and Ziemann, P. J.: Effect of the Hydroxyl Group on Yields and Composition of Organic Aerosol Formed from OH Radical-Initiated Reactions of Alcohols in the Presence of  $NO_x$ , ACS Earth Space Chem., 3, 413–423, <https://doi.org/10.1021/acsearthspacechem.9b00015>, 2019.

Chen, Y., Zheng, P., Wang, Z., Pu, W., Tan, Y., Yu, C., Xia, M., Wang, W., Guo, J., Huang, D., Yan, C., Nie, W., Ling, Z., Chen, Q., Lee, S., and Wang, T.: Secondary Formation and Impacts of Gaseous Nitro-Phenolic Compounds in the Continental Outflow Observed at a Background Site in South China, Environ. Sci. Technol., 56, 6933–6943, <https://doi.org/10.1021/acs.est.1c04596>, 2022.

Cheng, X., Chen, Q., Li, Y., Huang, G., Liu, Y., Lu, S., Zheng, Y., Qiu, W., Lu, K., Qiu, X., Bianchi, F., Yan, C., Yuan, B., Shao, M., Wang, Z., Canagaratna, M. R., Zhu, T., Wu, Y., and Zeng, L.: Secondary Production of Gaseous Nitrated Phenols in Polluted Urban Environments, Environ. Sci. Technol., 55, 4410–4419, <https://doi.org/10.1021/acs.est.0c07988>, 2021.

Dada, L., Stolzenburg, D., Simon, M., Fischer, L., Heinritzi, M., Wang, M., Xiao, M., Vogel, A. L., Ahonen, L., Amorim, A., Baalbaki, R., Baccarini, A., Baltensperger, U., Bianchi, F., Daellenbach, K. R., DeVivo, J., Dias, A., Dommen, J., Duplissy, J., Finkenzeller, H., Hansel, A., He, X.-C., Hofbauer, V., Hoyle, C. R., Kangasluoma, J., Kim, C., Kürten, A., Kvashnin, A., Mauldin, R., Makhmutov, V., Marten, R., Mentler, B., Nie, W., Petäjä, T., Quéléver, L. L. J., Saathoff, H., Tauber, C., Tome, A., Molteni, U., Volkamer, R., Wagner, R., Wagner, A. C., Wimmer, D., Winkler, P. M., Yan, C., Zha, Q., Rissanen, M., Gordon, H., Curtius, J., Worsnop, D. R., Lehtipalo, K., Donahue, N. M., Kirkby, J., El Haddad, I., and Kulmala, M.: Role of sesquiterpenes in biogenic new particle formation, Sci. Adv., 9, eadi5297, <https://doi.org/10.1126/sciadv.adi5297>, 2023.

Gao, L., Song, J., Mohr, C., Huang, W., Vallon, M., Jiang, F., Leisner, T., and Saathoff, H.: Kinetics, SOA yields, and chemical composition of secondary organic aerosol from  $\beta$ -caryophyllene ozonolysis with and without nitrogen oxides between 213 and 313 K, Atmos. Chem. Phys., 22, 6001–6020, <https://doi.org/10.5194/acp-22-6001-2022>, 2022.

Kirkby, J., Duplissy, J., Sengupta, K., Frege, C., Gordon, H., Williamson, C., Heinritzi,

M., Simon, M., Yan, C., Almeida, J., Tröstl, J., Nieminen, T., Ortega, I. K., Wagner, R., Adamov, A., Amorim, A., Bernhammer, A.-K., Bianchi, F., Breitenlechner, M., Brilke, S., Chen, X., Craven, J., Dias, A., Ehrhart, S., Flagan, R. C., Franchin, A., Fuchs, C., Guida, R., Hakala, J., Hoyle, C. R., Jokinen, T., Junninen, H., Kangasluoma, J., Kim, J., Krapf, M., Kürten, A., Laaksonen, A., Lehtipalo, K., Makhmutov, V., Mathot, S., Molteni, U., Onnela, A., Peräkylä, O., Piel, F., Petäjä, T., Praplan, A. P., Pringle, K., Rap, A., Richards, N. A. D., Riipinen, I., Rissanen, M. P., Rondo, L., Sarnela, N., Schobesberger, S., Scott, C. E., Seinfeld, J. H., Sipilä, M., Steiner, G., Stozhkov, Y., Stratmann, F., Tomé, A., Virtanen, A., Vogel, A. L., Wagner, A. C., Wagner, P. E., Weingartner, E., Wimmer, D., Winkler, P. M., Ye, P., Zhang, X., Hansel, A., Dommen, J., Donahue, N. M., Worsnop, D. R., Baltensperger, U., Kulmala, M., Carslaw, K. S., and Curtius, J.: Ion-induced nucleation of pure biogenic particles, *Nature*, 533, 521–526, <https://doi.org/10.1038/nature17953>, 2016.

Liu, Y., Nie, W., Li, Y., Ge, D., Liu, C., Xu, Z., Chen, L., Wang, T., Wang, L., Sun, P., Qi, X., Wang, J., Xu, Z., Yuan, J., Yan, C., Zhang, Y., Huang, D., Wang, Z., Donahue, N. M., Worsnop, D., Chi, X., Ehn, M., and Ding, A.: Formation of condensable organic vapors from anthropogenic and biogenic volatile organic compounds (VOCs) is strongly perturbed by NO<sub>x</sub> in eastern China, *Atmos. Chem. Phys.*, 21, 14789–14814, <https://doi.org/10.5194/acp-21-14789-2021>, 2021.

Liu, Y., Liu, C., Nie, W., Li, Y., Ge, D., Chen, L., Zhu, C., Wang, L., Zhang, Y., Liu, T., Qi, X., Wang, J., Huang, D., Wang, Z., Yan, C., Chi, X., and Ding, A.: Exploring condensable organic vapors and their co-occurrence with PM<sub>2.5</sub> and O<sub>3</sub> in winter in Eastern China, *Environ. Sci.: Atmos.*, 3, 282–297, <https://doi.org/10.1039/D2EA00143H>, 2023.

Luo, H., Vereecken, L., Shen, H., Kang, S., Pullinen, I., Hallquist, M., Fuchs, H., Wahner, A., Kiendler-Scharr, A., Mentel, T. F., and Zhao, D.: Formation of highly oxygenated organic molecules from the oxidation of limonene by OH radical: significant contribution of H-abstraction pathway, *Atmos. Chem. Phys.*, 23, 7297–7319, <https://doi.org/10.5194/acp-23-7297-2023>, 2023.

Massoli, P., Stark, H., Canagaratna, M. R., Krechmer, J. E., Xu, L., Ng, N. L., Mauldin, R. L. I., Yan, C., Kimmel, J., Misztal, P. K., Jimenez, J. L., Jayne, J. T., and Worsnop, D. R.: Ambient Measurements of Highly Oxidized Gas-Phase Molecules during the Southern Oxidant and Aerosol Study (SOAS) 2013, *ACS Earth Space Chem.*, 2, 653–672, <https://doi.org/10.1021/acsearthspacechem.8b00028>, 2018.

Mohr, C., Thornton, J. A., Heitto, A., Lopez-Hilfiker, F. D., Lutz, A., Riipinen, I., Hong, J., Donahue, N. M., Hallquist, M., Petäjä, T., Kulmala, M., and Yli-Juuti, T.: Molecular identification of organic vapors driving atmospheric nanoparticle growth, *Nat Commun*, 10, 4442, <https://doi.org/10.1038/s41467-019-12473-2>, 2019.

Nie, W., Yan, C., Huang, D. D., Wang, Z., Liu, Y., Qiao, X., Guo, Y., Tian, L., Zheng, P., Xu, Z., Li, Y., Xu, Z., Qi, X., Sun, P., Wang, J., Zheng, F., Li, X., Yin, R., Dallenbach,

K. R., Bianchi, F., Petäjä, T., Zhang, Y., Wang, M., Schervish, M., Wang, S., Qiao, L., Wang, Q., Zhou, M., Wang, H., Yu, C., Yao, D., Guo, H., Ye, P., Lee, S., Li, Y. J., Liu, Y., Chi, X., Kerminen, V.-M., Ehn, M., Donahue, N. M., Wang, T., Huang, C., Kulmala, M., Worsnop, D., Jiang, J., and Ding, A.: Secondary organic aerosol formed by condensing anthropogenic vapours over China's megacities, *Nat. Geosci.*, 15, 255–261, <https://doi.org/10.1038/s41561-022-00922-5>, 2022.

Richters, S., Herrmann, H., and Berndt, T.: Highly Oxidized RO<sub>2</sub> Radicals and Consecutive Products from the Ozonolysis of Three Sesquiterpenes, *Environ. Sci. Technol.*, 50, 2354–2362, <https://doi.org/10.1021/acs.est.5b05321>, 2016.

Song, K., Guo, S., Wang, H., Yu, Y., Wang, H., Tang, R., Xia, S., Gong, Y., Wan, Z., Lv, D., Tan, R., Zhu, W., Shen, R., Li, X., Yu, X., Chen, S., Zeng, L., and Huang, X.: Measurement report: Online measurement of gas-phase nitrated phenols utilizing a CI-LToF-MS: primary sources and secondary formation, *Atmos. Chem. Phys.*, 21, 7917–7932, <https://doi.org/10.5194/acp-21-7917-2021>, 2021.

Tsiliannis, E., Hammes, J., Salvador, C., Mentel, T., and Hallquist, M.: Effect of NO<sub>x</sub> on 1,3,5-trimethylbenzene (TMB) oxidation product distribution and particle formation, *Atmospheric Chemistry and Physics*, 19, 15073–15086, <https://doi.org/10.5194/ACP-19-15073-2019>, 2019.

Wang, Y., Mehra, A., Krechmer, J., Yang, G., Hu, X., Lu, Y., Lambe, A., Canagaratna, M., Chen, J., Worsnop, D., Coe, H., and Wang, L.: Oxygenated products formed from OH-initiated reactions of trimethylbenzene: autoxidation and accretion, *Atmospheric Chemistry and Physics*, null, null, <https://doi.org/10.5194/acp-2020-165>, 2020.

Wang, Z., Ehn, M., Rissanen, M., Garmash, O., Quéléver, L., Xing, L., Monge-Palacios, M., Rantala, P., Donahue, N., Berndt, T., and Sarathy, S. M.: Efficient alkane oxidation under combustion engine and atmospheric conditions, *Communications Chemistry*, 4, null, <https://doi.org/10.1038/s42004-020-00445-3>, 2021.

Wolfe, G. M., Marvin, M. R., Roberts, S. J., Travis, K. R., and Liao, J.: The Framework for 0-D Atmospheric Modeling (F0AM) v3.1, *Geosci. Model Dev.*, 9, 3309–3319, <https://doi.org/10.5194/gmd-9-3309-2016>, 2016.

Yan, C., Nie, W., Äijälä, M., Rissanen, M. P., Canagaratna, M. R., Massoli, P., Junninen, H., Jokinen, T., Sarnela, N., Häme, S. A. K., Schobesberger, S., Canonaco, F., Yao, L., Prévôt, A. S. H., Petäjä, T., Kulmala, M., Sipilä, M., Worsnop, D. R., and Ehn, M.: Source characterization of highly oxidized multifunctional compounds in a boreal forest environment using positive matrix factorization, *Atmospheric Chemistry and Physics*, 16, 12715–12731, <https://doi.org/10.5194/acp-16-12715-2016>, 2016.